IEEE Access
Multidisciplinary : Rapid Review : Open Access Journal

Received 23 September 2023, accepted 5 October 2023, date of publication 9 October 2023, date of current version 13 October 2023.

Digital Object Identifier 10.1109/ACCESS.2023.3322979

RESEARCH ARTICLE

A Compact Three-Port Antenna With Enhanced Inter-Port Isolation for Polarization and Pattern Diversity

JIHUN CHOI[1,2], (Member, IEEE), AND FIKADU T. DAGEFU[1], (Senior Member, IEEE)
[1]DEVCOM Army Research Laboratory, Adelphi, MD 20783, USA
[2]Booz Allen Hamilton Inc., McLean, VA 22102, USA

Corresponding author: Jihun Choi (choi_jihun@bah.com)

This work was supported by the U.S. Army Research Laboratory, Adelphi, MD, USA.

ABSTRACT This paper presents a compact three-port antenna design suitable for use in mobile radio systems that require polarization and pattern diversity. The antenna design utilizes a shorted bow-tie patch split in half with an air gap and a top-loaded two-element monopole placed along the gap on a small common ground plane ($0.37\lambda^2$) to achieve a compact form factor. The patch is excited by aperture coupling and probe feeding via two independent ports, producing two orthogonally polarized broadside patterns for polarization diversity. Meanwhile, the co-located monopole generates a vertically polarized omnidirectional pattern to provide pattern diversity. High inter-port isolation (> 25 dB) is achieved by incorporating simple decoupling structures shorted to the ground plane between the patch and the monopole. Measurements on the antenna prototype show that envelope correlation coefficients among the three different radiation patterns are lower than –37 dB (or 0.0002) within the operating bandwidth, making this antenna a good candidate for diversity applications.

INDEX TERMS Antenna diversity, monopole antenna, patch antenna, pattern diversity, polarization diversity, port isolation.

I. INTRODUCTION

Polarization and pattern diversity techniques have revolutionized the development of compact wireless systems by allowing multiple antennas to be placed in close proximity while improving signal quality and link reliability [1]. However, co-locating multi-port antennas that enable both diversity techniques in a small form factor poses a challenge. In particular, using a smaller common ground plane to achieve a more compact antenna design can significantly reduce port-to-port isolation, which is crucial for the independent operation of each radiating element. Additionally, the reduced radiation efficiency and operating bandwidth resulting from a smaller ground plane becoming an integral part of the antenna can be a concern [2]. The inter-port isolation, which is primarily affected by mutual coupling resulting from the currents induced on the small common ground plane, as well as near-field coupling from closely spaced antenna elements, is an important parameter for multi-port antenna design. To meet the requirement of practical applications of compact multi-port antennas, which typically demand inter-port isolation greater than 20 dB, an effective method of reducing mutual coupling is necessary.

Various approaches have been introduced to reduce mutual coupling among the antenna elements within multi-port antenna systems [3], [4], [5], [6]. These approaches typically involve inserting lumped and/or distributed elements or modifying the ground plane between coupled antenna elements. For instance, a decoupling network composed of two parallel transmission lines and a shunt reactive component can be inserted between closely spaced printed monopole antennas and their input ports to improve port-to-port isolation, as described in [4]. Another technique utilizes multiple slits interleaved with strips on the ground plane, which act as a band-stop filter, to reduce mutual coupling between closely packed monopoles or patches,

The associate editor coordinating the review of this manuscript and approving it for publication was Julien Sarrazin.

as detailed in [5]. However, these techniques often require a relatively large space and increase design complexity. Other methods, including electromagnetic band-gap structures and defected ground structures, have also been proposed for mutual coupling reduction, but they face similar limitations. Therefore, there is a need for new approaches that can effectively reduce mutual coupling while minimizing design complexity and space requirements.

The goal of this paper is to present a compact three-port antenna design for low-power, low-rate, wireless networking at the 915 MHz ISM band that provides both polarization and pattern diversity while maintaining high inter-port isolation and compactness. The proposed design can be integrated into multiple-input multiple-output (MIMO) systems, where multiple antennas are used for simultaneous data transmission and reception. In such systems, the diversity antenna contributes to increased data throughput, improved link reliability, and better overall performance especially in rich multi-path environments (e.g., urban and indoor settings) as shown in [7]. Moreover, the antenna can be used for low probability of detection (LPD) communication applications as outlined in [8]. Its distinctive tri-polarization diversity attributes can substantially reduce the probability of detection at an adversary node, while crucial data streams are transmitted and received across the distinct polarization channels established between friendly nodes.

The design features a shorted bow-tie patch that is split into two halves and a top-loaded, two-element monopole co-located on a small common ground plane ($0.37\lambda^2$) to achieve compactness. Exciting the patch through two independent ports with aperture coupling and probe feeding produces two orthogonally polarized broadside radiation patterns, while the co-located monopole produces a vertically polarized omnidirectional pattern. To achieve high inter-port isolation in this compact design, the antenna incorporates simple decoupling elements that require minimal space and do not require any ground plane modification. These elements significantly reduce mutual coupling between the antenna elements with minimal degradation of their radiation performance. The proposed antenna achieves greater compactness and higher inter-port isolation within the given dimensions, including the ground plane, compared to existing three-port diversity antennas [9], [10], [11], [12], [13], [14], [15], [16], [17].

The rest of the paper is organized as follows. Section II introduces the proposed antenna design approach and a method to enhance the inter-port isolation. Section III presents the performance analysis of the proposed antenna via simulations and measurements, along with an evaluation of its diversity performance by means of the envelope correlation coefficient and the diversity gain.

II. ANTENNA DESIGN

A. DESIGN APPROACH

The proposed antenna design is based on the principle of co-locating antennas on a common ground plane in a location where minimal mutual coupling occurs. To illustrate this, consider a conventional half-wave microstrip patch and a quarter-wave monopole antenna, as shown in Fig. 1. At the center of the patch, the electric field is null and the electric current is at a maximum, resulting in a theoretically zero impedance. By placing the monopole antenna at the center of the patch, low mutual coupling can be achieved between the two antennas. While pattern diversity is realized by producing broadside and omnidirectional radiation patterns from the patch and the monopole, respectively, polarization diversity can also be achieved by employing two different feeds exciting the patch. Here, orthogonally polarized fields from the patch can be generated by positioning the feeds with a 90-degree separation.

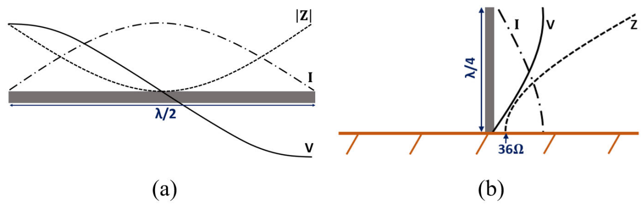

FIGURE 1. Current, voltage, and impedance distribution on (a) a conventional half-wave microstrip patch antenna and (b) a quarter-wave monopole antenna.

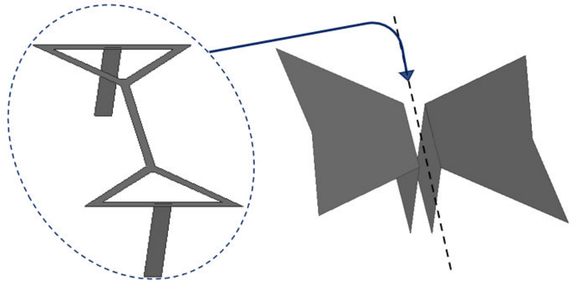

FIGURE 2. A design approach to co-locate an electrically short, top-loaded, two-element monopole (left) and a compact bow-tie patch split into two with shorting plates (right) on a small common ground plane.

Fig. 2 depicts the proposed method for designing a polarization and pattern diversity antenna in a compact form factor, which applies the aforementioned principle. The design consists of two compact radiating elements. First, a bow-tie patch split into two using shorting plates is introduced [18]. Here, the shorting plates are placed along the center where the current is maximum and the voltage (electric field) is zero, producing strong magnetic coupling between them; when one of the patch segments is excited, the other is parasitically coupled. Consequently, the current distribution on the patch is least altered and thus similar to that of the conventional patch, while achieving a significant size reduction. Second, an electrically short, top-loaded, two-element monopole [19], [20] is introduced to substantially reduce the overall profile of the design as compared with the conventional quarter-wave monopole. This monopole

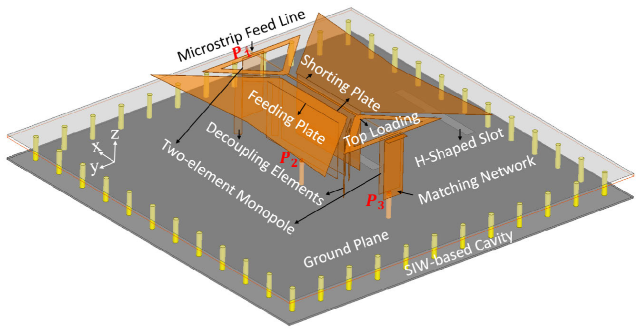

(a)

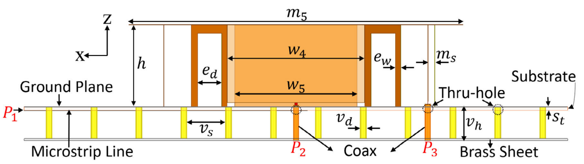

(b)

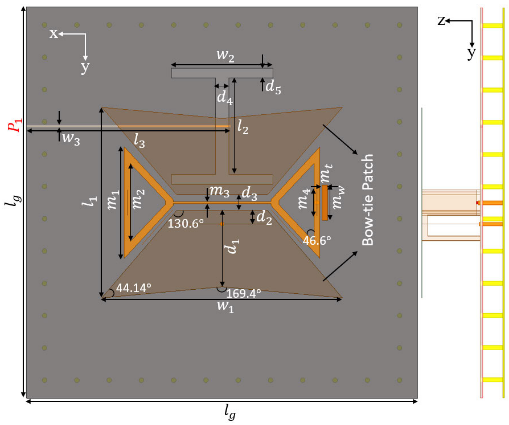

(c)

FIGURE 3. Geometry of the proposed three-port diversity antenna: (a) Perspective view, (b) side view, and (c) top and front view. An outer conductor of the coax for both P_2 and P_3, along with the array of short metal rods forming the SIW cavity, is connected to the ground plane and the bottom brass sheet via thru-holes. The decoupling elements are directly connected to the ground plane with both ends shorted to it. Parameter values used in the simulation are $l_g = 200$, $l_1 = 97.4$, $l_2 = 42.4$, $l_3 = 104.7$, $w_1 = 123$, $w_2 = 42.5$, $w_3 = 1.1$, $w_4 = 50.4$, $w_5 = 45$, $d_1 = 38.8$, $d_2 = 6.8$, $d_3 = 8.4$, $d_4 = 7$, $d_5 = 5$, $m_1 = 57$, $m_2 = 40$, $m_3 = 1$, $m_4 = 13.3$, $m_5 = 100$, $m_w = 11.2$, $m_t = 3$, $m_s = 2.5$, $e_w = 3.4$, $e_d = 13.1$, $v_h = 11.6$, $v_d = 2.4$, $v_s = 14.1$, $h = 30$, and $s_t = 1.3$ (all dimensions are in millimeters).

produces in-phase currents flowing through its two vertical elements, leading to an increase in effective height and thus enhanced gain compared to a single monopole with the same height. Once the common ground plane size for the design has been determined for integration into small mobile platforms such as unmanned ground vehicles (UGVs) and unmanned aerial vehicles (UAVs), careful selection of proper feeding networks for each radiating element, as well as their corresponding locations, is undertaken. Subsequently, design optimization is conducted to enhance the overall performance of the antenna.

Fig. 3 shows the geometry of the complete antenna design highlighting its dimension parameters and feeding ports ($P_{1,2,3}$). The initial dimensions of the radiating elements in the proposed design were derived from prior research [18], [19], [20]. For instance, the initial length (l_1) of the shorted bow-tie patch was selected to be approximately 0.25λ at its resonance [18]. Similarly, the capacitive top loading of the two-element monopole was determined using an equivalent circuit model of a multi-element monopole antenna known as a modified T-type 180-degree phase shifter, as discussed in [19] and [20], for a given height. Starting with the selection of the initial dimensions, design optimization processes based on full-wave electromagnetic simulations were conducted to determine the final antenna dimensions for achieving the desired antenna performance.

The bow-tie patch element, whose dimensions are 0.375λ × 0.297λ at 915 MHz, is positioned over the common ground plane (0.61λ × 0.61λ or 0.37λ^2) without any dielectric materials in between to achieve higher bandwidth. The probe feed and the aperture-coupled feed are adopted to produce orthogonal polarization from the patch. The probe feed is located close to the center of a patch segment, which facilitates the mutual coupling reduction between the patch and the monopole. The aperture feed arranged orthogonally to the probe feed is located under the other patch segment and transmits energy to the patch through an H-shaped slot etched on the ground plane. A microstrip feed line for the aperture-coupled feed is positioned under the ground plane spaced with a substrate having a dielectric constant of 9.56. The top-loaded two-element monopole, with a height of 0.09λ, is positioned along the air gap between the two segments of the bow-tie patch element. The top loading of the monopole and the patch are designed to lie on the same plane in the air.

B. DESIGN OPTIMIZATION

Input impedance and resonant frequency of the patch antenna fed by the aperture coupling are optimized by adjusting the slot length l_2 (w_2) and width d_4 (d_5) along with the length of the tuning stub, the feed line extending beyond the coupling slot. Likewise, those of the patch fed by the probe are determined by choosing the feeding plate width w_4 and its position d_2. In addition, parasitic coupling between the patch and the monopole caused by the surface currents flowing through the patch and the top loading of the monopole is controlled, to some extent, by the air gap separating the two patch segments d_3 and/or the width of the top loading m_3. Note that altering d_3 also affects the resonant frequency and bandwidth of the patch antenna resulting from the change in the overall antenna dimension and the level of magnetic coupling between the shorting plates. The resonant frequency of the monopole antenna for a given height is tuned by changing the slot dimensions on its top loading. This change is also responsible for the amount of parasitic in-plane coupling. Impedance matching of the monopole is improved by placing a vertical element with a small top hat adjacent to its feed. Here, the added vertical element contributes little to the radiation from the monopole since only a small fraction of the current flows through it.

A substrate-integrated waveguide (SIW)-based cavity [21] is included in the design to enhance the front-to-back ratio (FBR) of the patch antenna at P_1 by effectively suppressing unwanted electromagnetic radiation in the backward direction from the H-shaped slot on the small ground plane. The SIW cavity is formed by placing an additional metal plate underneath the antenna ground plane and connecting it to the ground plane through an array of short metal rods with an air gap between them. Here, the array of metallic rods in the SIW cavity acts as a shield, blocking and attenuating radiation from the patch element and the aperture feed that would otherwise propagate in undesired directions. As a result, electromagnetic energy is redirected and focused in the forward direction, significantly improving the FBR along with radiation efficiency. The SIW cavity also enables a compact design with a smaller volume as well as reduced fabrication complexity compared to other methods using a metallic reflector element or a metallic cavity.

C. INTER-PORT ISOLATION ENHANCEMENT

As previously mentioned, ensuring a high level of inter-port isolation is a crucial aspect of multi-port antenna design. A preliminary study [22] shows that the antenna design without decoupling elements exhibits relatively low port isolation between P_2 and P_3 (> 14 dB), compared to that between P_1 and P_2 (> 43 dB), and P_1 and P_3 (> 28 dB), over a common impedance bandwidth. To further enhance the P_2-to-P_3 isolation to fulfill the demanding requirements of practical applications (> 20 dB), an effective decoupling method is proposed that does not require modifications to the ground plane. The method involves inserting a pair of metallic structures, with their ends shorted to the ground plane, between one of the patch segments and the top loading of the monopole antenna. These structures mitigate mutual coupling effects between the antenna elements by partly canceling out induced currents from near-field coupling and the common ground plane when P_2 and P_3 are excited. The antenna radiation performance is minimally affected by the decoupling structures.

Fig. 4(a) and (b) illustrate the vector surface current distribution overlaid on a transparent view of the proposed antenna without decoupling elements where the vector directions are indicated with short arrows for P_2 and P_3 excitation, respectively. Here, the red arrows indicate the currents when the patch is excited at P_2 or the monopole is excited at P_3, while the black arrows represent the currents induced from the near-field coupling and the common ground plane. When P_2 is excited, the induced currents (black arrows) on both vertical elements of the monopole antenna are 180-degrees out-of-phase with respect to the excited current (red arrows) on the feeding plate of the patch. When P_3 is excited, the currents (black arrows) induced on both the shorting plates of the patch are in-phase (and thus the currents induced on each patch segment are 180-degrees out-of-phase with each other) relative to the excited currents (red arrows) on the vertical elements of the monopole. Since in-phase currents in the vertical direction are a major source of radiated fields for the monopole, the induced currents on its vertical elements from P_2 excitation (and those on the shorting plates of the patch from P_3 excitation) should be suppressed to reduce the mutual coupling effect. As depicted in Fig. 4(c) and (d), the addition of the decoupling structures gives rise to the induced currents in each case above that are 180-degrees out-of-phase with each other, facilitating a significant mutual coupling reduction between the patch and the monopole.

III. PERFORMANCE ANALYSIS AND EVALUATION

A. ANTENNA MEASUREMENT AND ANALYSIS

To validate the proposed design, a prototype antenna operating within the 915-MHz ISM band was fabricated and tested (its top view and side view are shown in Fig. 5). A semi-rigid coaxial cable terminated with a 50-Ohm SMA connector is used to feed the antenna at P_2 and P_3. To enhance the mechanical stability of the antenna structure, a spacer composed of Styrofoam is inserted between the patch/top loading of the monopole and the ground plane.

Reflection coefficients and inter-port isolations of the prototype were measured with a calibrated two-port vector network analyzer (VNA). Two out of three antenna ports were connected to each port of the VNA while the remaining one was terminated with a 50-Ohm load. Fig. 6 shows measured and simulated reflection coefficients of the antenna prototype as a function of frequency. A shift in the center frequency of the prototype (910 MHz) is observed compared with the simulated one (915 MHz). This is mainly due to fabrication errors. Measured (simulated) impedance bandwidths of the three-port antenna are 18 (16.5), 31.2 (32), and 105 (109) MHz at P_1, P_2, and P_3, respectively. Fig. 7 depicts measured inter-port isolations of the prototype in comparison with the simulated ones. The measured (simulated) isolation between P_1 and P_2, P_1 and P_3, and P_2 and P_3, within the common bandwidth, are higher than 30.4 (37.4), 30.1 (35.7), and 25 (26) dB, respectively. Compared to the antenna design without the decoupling elements, the isolation between P_2 and P_3 is improved by more than 11 dB.

Next, far-field radiation patterns and gains of the prototype antenna were measured in an RF anechoic chamber. The measurements were conducted by exciting one port while the others were terminated with 50-Ohm loads. Fig. 8 illustrates the measured and simulated 2D radiation patterns of the antenna prototype in the principal planes. For reference, the simulated 3D radiation patterns of the antenna are also presented in Fig. 9. The measurement results are in good agreement with the simulated ones. The antenna produces orthogonally polarized broadside radiation patterns with the measured (simulated) peak gain of 6.1 (6) dBi at P_1 and 7.9 (8) dBi at P_2. On the other hand, a nearly omnidirectional radiation pattern with the measured (simulated) peak gain of 3.8 (2.8) dBi is produced from the antenna at P_3. The

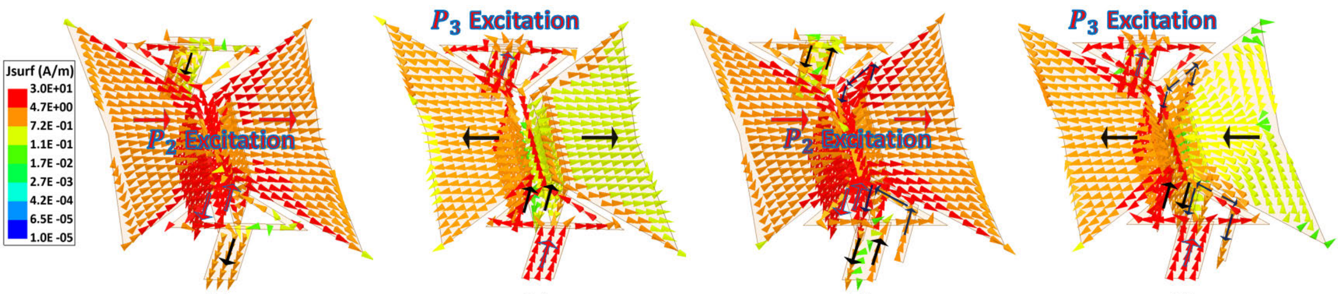

(a) (b) (c) (d)

FIGURE 4. Vector surface current distribution on the proposed antenna without ((a) and (b)) and with decoupling elements ((c) and (d)).

TABLE 1. The electrical size and measured performance of the proposed prototype compared with those of existing three-port diversity antennas.

	Center Freq. (GHz)	Ground Plane Size (λ^2)	Antenna Height above Ground Plane (λ)	Antenna Size (Largest Dimension in λ)	Inter-port Isolation (dB)	Common FBW (%)	Peak Gain (dBi)
[9]	5.9	5.12	0.06	0.48	35	2.3	9.4, 6.4
[10]	2.6	3.76	0.24	0.75	20	2.8	9.5, 10.5, 2.9
[11]	5.8	1.35	0.06	0.68	15	2.9	5.7, 3.6
[12]	2.45	1.32	0.26	0.43	24	4.5	2.5, 2.5, 2.3
[13]	5.8	1.26	0.06	0.57	16	1.7	6.7, 5.7
[14]	5	1.07	0.09	0.72	15	13.9	11.2, 10.8, 5.8
[15]	2.3	0.83	0.07	0.97	20	13.2	8.6, 8.6, 3.2
[16]	2.5	0.61	0.08	0.33	16	7.6	NA
[17]	2.44	0.24	0.05	0.31	13.5	3.5	3.8, 3.8, –0.9
This work	0.915	0.37	0.09	0.48	25	2.0	6.1, 7.9, 3.8

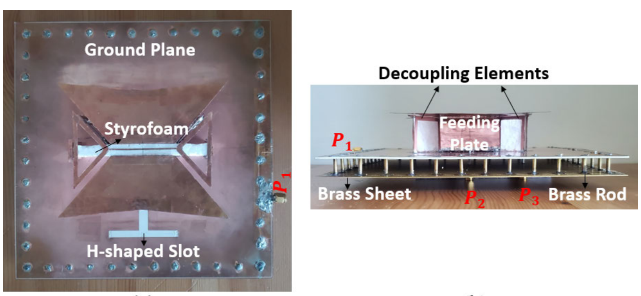

(a) (b)

FIGURE 5. Fabricated antenna prototype: (a) Top view and (b) side view.

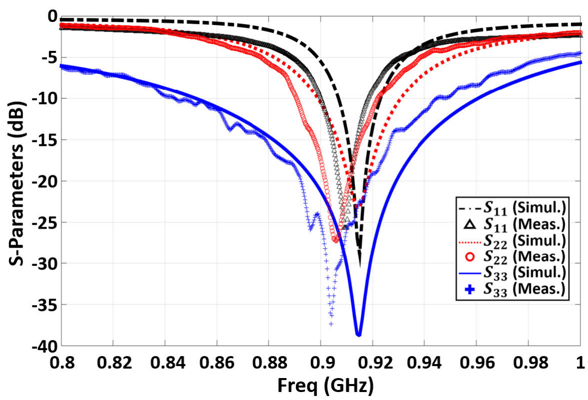

FIGURE 6. Measured reflection coefficients of the proposed diversity antenna as a function of frequency, compared with simulated ones.

measured (simulated) cross-polarization levels of the antenna at each port where the maximum gain occurs are –28.0 (–32.7), –36.2 (–38.1), –18 (–22) dB, respectively. The measured (simulated) FBR of the patch at P_1 and P_2 are 17 (17.8) and 11 (11.2) dB, respectively. The addition of the SIW-based cavity improves the FBR of the patch fed through aperture coupling by more than 15 dB.

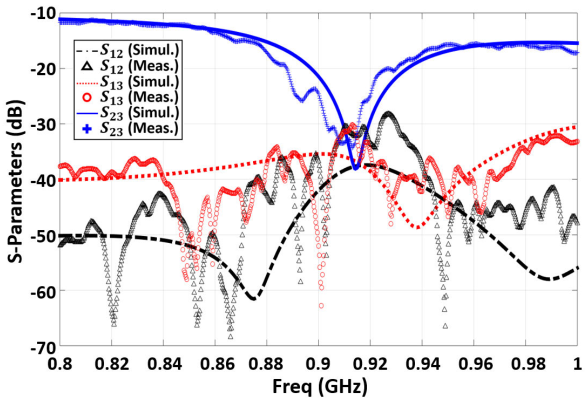

FIGURE 7. **Measured inter-port isolations of the proposed diversity antenna as a function of frequency, compared with simulated ones.**

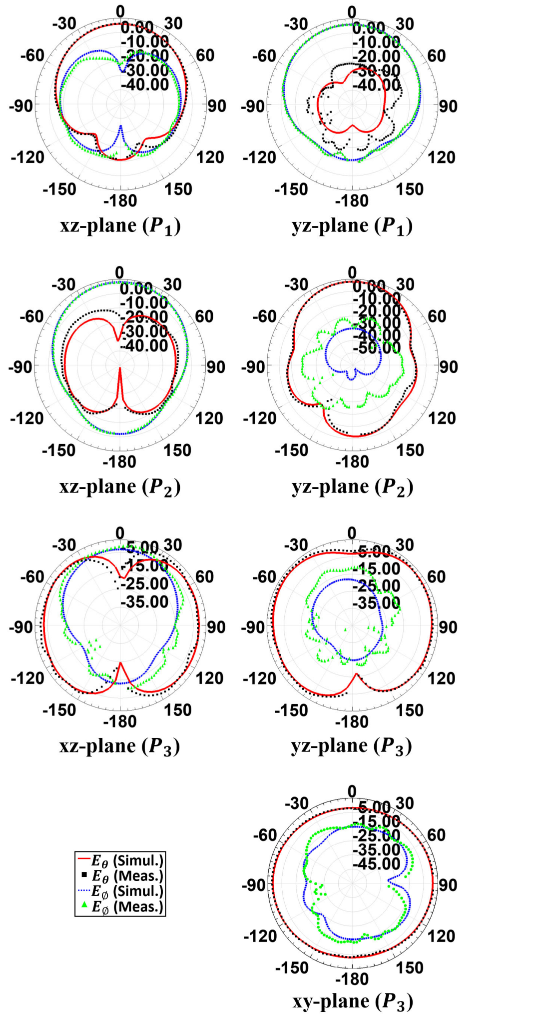

FIGURE 8. **Measured 2D radiation patterns of the proposed diversity antenna at 910 MHz. Simulated results are also plotted for comparison.**

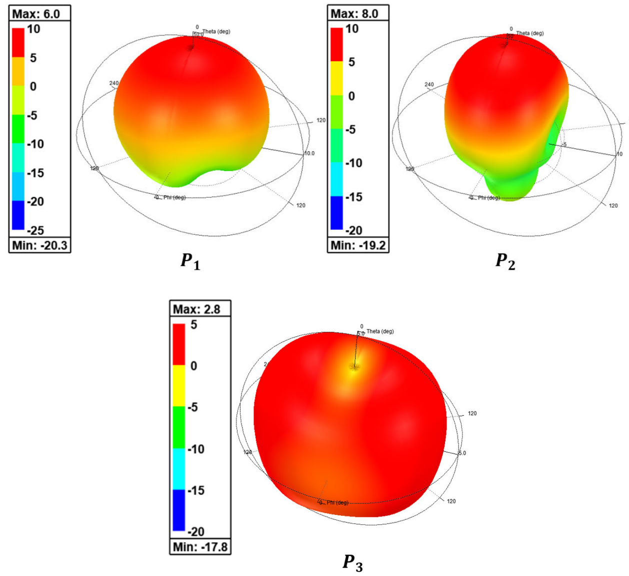

FIGURE 9. **Simulated 3D radiation patterns of the proposed diversity antenna at 915 MHz.**

Table 1 provides a comprehensive comparison of the electrical size and measured performance of the proposed prototype with existing three-port diversity antennas [9], [10], [11], [12], [13], [14], [15], [16], [17]. The proposed antenna design effectively achieves a dual goal of enhancing compactness and maximizing inter-port isolation within the given dimensions including the ground plane, surpassing other designs. For instance, while [9] and [12] achieve comparable or higher inter-port isolation, they require significantly larger ground plane sizes. In contrast, the proposed antenna achieves comparable or slightly lower common fractional bandwidth (FBW) and gain, yet exhibits up to 10 dB higher inter-port isolation despite its smaller size compared to [10], [11], and [13]. Similarly, [14], [15], and [16] feature a larger form factor and up to 10 dB lower inter-port isolation, even though they offer a broader FBW compared to the proposed antenna. The only design with a smaller ground plane than the proposed antenna is [17], but it compromises with over 11.5 dB lower inter-port isolation and significantly less gain. Therefore, when considering integration into small mobile platforms such as UGVs and UAVs with limited ground plane size, the proposed antenna emerges as the optimal choice. It not only fulfills the inter-port isolation requirements (> 20 dB) for practical multi-port antenna applications but also demonstrates superior compactness.

While the incorporation of the SIW cavity into the antenna design improves the FBR, it comes at the cost of reducing the common FBW, creating a trade-off between the two performance metrics. The proposed antenna with the SIW cavity has a narrower FBW (2 % measured/ 1.8 % simulated), compared to that (3.2 %) of the design without the SIW cavity (its inter-port isolation and peak gain are 22 dB and 4.3, 8.0, 3.0 dBi, respectively, obtained from simulations). It's worth noting that the proposed antenna is optimized for low-power, low-rate wireless networking as mentioned earlier, so the reduced bandwidth may not be an issue in certain applications. However, for broader band operation,

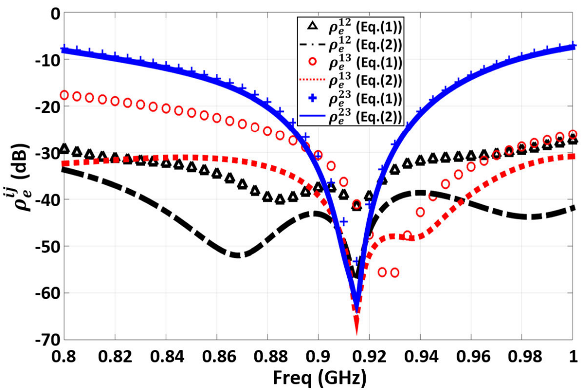

FIGURE 10. Envelope correlation coefficient ρ_e^{ij} computed by two different methods using simulation data as a function of frequency.

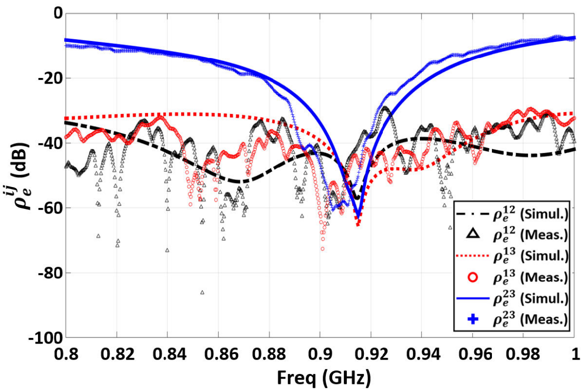

FIGURE 11. Envelope correlation coefficient ρ_e^{ij} computed with simulated and measured S-parameter data as a function of frequency.

a stacked patch configuration [23] can be applied to the SIW cavity-backed antenna. This configuration involves coupling a driven patch to a vertically stacked patch, resulting in a double resonance response that can increase the antenna's overall bandwidth.

B. DIVERSITY PERFORMANCE EVALUATION

As crucial metrics to evaluate the performance of diversity antennas for wireless communications, envelope correlation coefficient (ECC) and diversity gain are commonly used. Assuming an isotropic propagation environment, the ECC ρ_e^{ij} (i,j = 1, 2, 3 and i $\neq$ j), a measure of similarity between two radiation patterns characterizing the degree of correlation between the communication channels, can be computed as [24]

$$\rho_e^{ij} = \frac{|\iint \overline{F_i(\theta,\phi)} \cdot \overline{F_j^*(\theta,\phi)}\, d\Omega|^2}{\iint |\overline{F_i(\theta,\phi)}|^2\, d\Omega \iint |\overline{F_j(\theta,\phi)}|^2\, d\Omega}, \tag{1}$$

where $\overline{F_{i(j)}(\theta,\phi)} = \hat{\theta}F_\theta^{i(j)}(\theta,\phi) + \hat{\phi}F_\phi^{i(j)}(\theta,\phi)$ (i,j = 1, 2, 3 and i $\neq$ j), complex values of the far-field radiation patterns when the antenna is excited at port $i(j)$, and * denotes complex conjugate. This computation requires considerable efforts to collect the far-field data at frequencies of interest from either full-wave simulation or measurement. In [25], a simpler way of estimating the ECC using complex S-parameter data for lossless antennas in an isotropic propagation environment is introduced, which is given by

$$\rho_e^{ij} = \frac{|S_{ii}^* S_{ij} + S_{ji}^* S_{jj}|^2}{(1 - |S_{ii}|^2 - |S_{ji}|^2)(1 - |S_{jj}|^2 - |S_{ij}|^2)}. \tag{2}$$

Fig. 10 shows the ECCs of the proposed diversity antenna computed by (1) and (2), respectively, as a function of frequency. The results obtained from the two different methods agree with each other in which ρ_e^{ij} < -33 dB (or 0.0005) and ρ_e^{ij} < -38 dB (or 0.00016) from (1) and (2), respectively, within the common impedance bandwidth of the antenna.

In order to estimate the ECC of the fabricated prototype antenna, the simpler method by (2) using measured complex S-parameter data is adopted. Fig. 11 illustrates its corresponding results for the ECC of the antenna prototype, together with those computed with the simulated S-parameters in Fig. 10 for comparison. The results show a similar trend in which ρ_e^{ij} computed using the measured data is below –37 dB (or 0.0002) over the common impedance bandwidth.

Diversity gain is a measure of the improvement in signal-to-interference ratio obtained from the diversity antenna system compared to a single-element antenna system. As described in [26], it can be calculated as $G_{div} = G_0\sqrt{1 - \rho_e^{ij}}$ where G_0 is the gain when the signals from the diversity antenna are not correlated, and its value is determined by modulation and diversity schemes and outage probability (e.g., G_0= 10 at 1 % outage probability using selection combining). As a result of very low ρ_e^{ij}, the diversity gain of the proposed antenna nearly approaches G_0 over its common impedance bandwidth.

IV. CONCLUSION

A compact, three-port diversity antenna with high inter-port isolation is presented for low-power, low-rate, wireless networks. The antenna design allows for both polarization and pattern diversity, realized by co-locating a shorted bow-tie patch split in half and a top-loaded, two-element monopole on a small common ground plane. The proposed antenna achieves high inter-port isolation within the given dimensions by utilizing space-efficient decoupling structures while maintaining its radiation performance. A prototype of the antenna was fabricated, and the design was validated through measurements. The antenna provides excellent diversity performance over the operating band, evaluated using the envelope correlation coefficient and diversity gain, and thus is best suited for diversity applications requiring compact radio systems.

REFERENCES

[1] P. M. C. Nathan, *Wireless communications*. New Delhi, India: PHI Learning, 2008.
[2] S. R. Best, "The significance of ground-plane size and antenna location in establishing the performance of ground-plane-dependent antennas," *IEEE Antennas Propag. Mag.*, vol. 51, no. 6, pp. 29–43, Dec. 2009.

[3] I. Nadeem and D.-Y. Choi, "Study on mutual coupling reduction technique for MIMO antennas," *IEEE Access*, vol. 7, pp. 563–586, 2019.
[4] S.-C. Chen, Y.-S. Wang, and S.-J. Chung, "A decoupling technique for increasing the port isolation between two strongly coupled antennas," *IEEE Trans. Antennas Propag.*, vol. 56, no. 12, pp. 3650–3658, Dec. 2008.
[5] C.-Y. Chiu, C.-H. Cheng, R. D. Murch, and C. R. Rowell, "Reduction of mutual coupling between closely-packed antenna elements," *IEEE Trans. Antennas Propag.*, vol. 55, no. 6, pp. 1732–1738, Jun. 2007.
[6] S. Dey, S. Dey, and S. K. Koul, "Isolation improvement of MIMO antenna using novel EBG and hair-pin shaped DGS at 5G millimeter wave band," *IEEE Access*, vol. 9, pp. 162820–162834, 2021.
[7] F. T. Dagefu, J. Oh, J. Choi, and K. Sarabandi, "Measurements and physics-based analysis of co-located antenna pattern diversity system," *IEEE Trans. Antennas Propag.*, vol. 61, no. 11, pp. 5724–5734, Nov. 2013.
[8] C. Koumpouzi, F. T. Dagefu, J. Choi, J. Kong, and P. Spasojevic, "Exploiting polarization diversity to improve cyclostationary-based LPD properties of CDMA," *IEEE Wireless Commun. Lett.*, vol. 12, no. 1, pp. 6–10, Jan. 2023.
[9] N. P. Lawrence, C. Fumeaux, and D. Abbott, "Planar triorthogonal diversity slot antenna," *IEEE Trans. Antennas Propag.*, vol. 65, no. 3, pp. 1416–1421, Mar. 2017.
[10] K. Saurav, N. K. Mallat, and Y. M. M. Antar, "A three-port polarization and pattern diversity ring antenna," *IEEE Antennas Wireless Propag. Lett.*, vol. 17, no. 7, pp. 1324–1328, Jul. 2018.
[11] Y. Zheng and S. Yan, "A low-profile half-mode annular microstrip antenna with pattern diversity," *IEEE Antennas Wireless Propag. Lett.*, vol. 19, no. 10, pp. 1739–1743, Oct. 2020.
[12] X. S. Fang, K. W. Leung, and K. M. Luk, "Theory and experiment of three-port polarization-diversity cylindrical dielectric resonator antenna," *IEEE Trans. Antennas Propag.*, vol. 62, no. 10, pp. 4945–4951, Oct. 2014.
[13] A. A. Serra, A. R. Guraliuc, P. Nepa, G. Manara, I. Khan, and P. S. Hall, "Dual-polarisation and dual-pattern planar antenna for diversity in body-centric communications," *IET Microw., Antennas Propag.*, vol. 4, no. 1, pp. 106–112, 2010.
[14] K. Zhang, Z. H. Jiang, W. Hong, and D. H. Werner, "A low-profile and wideband triple-mode antenna for wireless body area network concurrent on-/off-body communications," *IEEE Trans. Antennas Propag.*, vol. 68, no. 3, pp. 1982–1994, Mar. 2020.
[15] Y. Zhang, K. Wei, Z. Zhang, and Z. Feng, "A broadband patch antenna with tripolarization using quasi-cross-slot and capacitive coupling feed," *IEEE Antennas Wireless Propag. Lett.*, vol. 12, pp. 832–835, 2013.
[16] H. Zhong, Z. Zhang, W. Chen, Z. Feng, and M. F. Iskander, "A tripolarization antenna fed by proximity coupling and probe," *IEEE Antennas Wireless Propag. Lett.*, vol. 8, pp. 465–467, 2009.
[17] S. Yan and G. A. E. Vandenbosch, "Wearable antenna with tripolarisation diversity for WBAN communications," *Electron. Lett.*, vol. 52, no. 7, pp. 500–502, Apr. 2016.
[18] J. Oh and K. Sarabandi, "Compact, low profile, common aperture polarization, and pattern diversity antennas," *IEEE Trans. Antennas Propag.*, vol. 62, no. 2, pp. 569–576, Feb. 2014.
[19] J. Oh, J. Choi, F. T. Dagefu, and K. Sarabandi, "Extremely small two-element monopole antenna for HF band applications," *IEEE Trans. Antennas Propag.*, vol. 61, no. 6, pp. 2991–2999, Jun. 2013.
[20] J. Choi and F. T. Dagefu, "A low-profile, top-loaded, multielement, monopole antenna for compact UGV systems," *IEEE Trans. Antennas Propag.*, vol. 70, no. 3, pp. 2277–2282, Mar. 2022.
[21] G. Q. Luo, Z. F. Hu, L. X. Dong, and L. L. Sun, "Planar slot antenna backed by substrate integrated waveguide cavity," *IEEE Antennas Wireless Propag. Lett.*, vol. 7, pp. 236–239, 2008.
[22] J. Choi and F. T. Dagefu, "A low-profile three-port antenna for compact polarization and pattern diversity systems," in *Proc. IEEE Int. Symp. Antennas Propag. USNC-URSI Radio Sci. Meeting (APS/URSI)*, Dec. 2021, pp. 493–494.
[23] S. Gao, L. W. Li, M. S. Leong, and T. S. Yeo, "A broad-band dual-polarized microstrip patch antenna with aperture coupling," *IEEE Trans. Antennas Propag.*, vol. 51, no. 4, pp. 898–900, Apr. 2003.
[24] R. G. Vaughan and J. B. Andersen, "Antenna diversity in mobile communications," *IEEE Trans. Veh. Technol.*, vol. VT-36, no. 4, pp. 149–172, Nov. 1987.
[25] S. Blanch, J. Romeu, and I. Corbella, "Exact representation of antenna system diversity performance from input parameter description," *Electron. Lett.*, vol. 39, no. 9, pp. 705–707, 2003.
[26] T.-S. Chu and L. J. Greenstein, "A semi-empirical representation of antenna diversity gain at cellular and PCS base stations," *IEEE Trans. Commun.*, vol. 45, no. 6, pp. 644–646, Jun. 1997.

JIHUN CHOI (Member, IEEE) received the B.S. degree in electrical engineering from Incheon National University, South Korea, in 2010, and the M.S. and Ph.D. degrees in electrical and computer engineering from the University of Michigan, Ann Arbor, MI, USA, in 2013 and 2017, respectively.

He is currently a Research Scientist with Booz Allen Hamilton Inc., McLean, VA, USA, and the DEVCOM U.S. Army Research Laboratory (ARL), Adelphi, MD, USA. His research interests include antenna miniaturization, antenna measurement techniques, wave propagation modeling in highly cluttered scenarios, and low-power HF/VHF radio system design.

FIKADU T. DAGEFU (Senior Member, IEEE) received the B.S. degree in electrical engineering from The University of Texas at Austin, in 2007, and the M.S. and Ph.D. degrees in electrical engineering from the University of Michigan, Ann Arbor, in 2009 and 2012, respectively. He is currently a Research Scientist with the U.S. Army Research Laboratory, Adelphi, MD, USA. His research interests include wireless channel modeling, small antennas, optical communications, and heterogeneous networking. He serves as an Associate Editor for IEEE Antennas and Wireless Propagation Letters and *Radio Science Letters* (RSL). Recently, he served as the Committee Chair for the 2023 IEEE International Symposium on Antennas and Propagation and USNC-URSI Radio Science Meeting (APS/URSI 2023) and the Track Chair for IEEE Military Communications Conference (MILCOM 2023).